# Structural Aspects of the Ambient-Pressure BEDT-TTF Superconductors

**Hideki Yamochi,*,† Tokutaro Komatsu,† Nozomu Matsukawa,† Gunzi Saito,† Takehiko Mori,‡ Masami Kusunoki,§ and Ken-ichi Sakaguchi§**

*Contribution from the Department of Chemistry, Faculty of Science, Kyoto University, Sakyo-ku, Kyoto 606-01, Japan, Institute for Molecular Science, Okazaki 444, Japan, and Institute for Protein Research, Osaka University, Yamadaoka, Suita, Osaka 565, Japan*

*Received May 12, 1993*®

**Abstract:** The crystal structures of two bis(ethylenedithio)tetrathiafulvalene (BEDT-TTF) superconductors, κ-(BEDT-TTF)$_2$Cu(CN)[N(CN)$_2$] and κ′-(BEDT-TTF)$_2$Cu$_2$(CN)$_3$ have been determined. From this analysis, empirical rules have been formulated which can predict the donor packing motif and superconducting transition temperatures of ambient-pressure BEDT-TTF superconductors with planar anions. These rules show that the packing of the donor molecules is governed by a pattern of "cores" of openings in the anion layer. We find superconducting transition temperatures are roughly proportional to the volume of the space in which the carrier can delocalize effectively.

## Introduction

From studies of charge-transfer complexes and radical salts as organic conductors, almost 50 different superconductors are presently known.[1,2] It has been found that the superconducting transition temperatures ($T_c$'s) can be increased by the selection of the counterion. Also, the choice of conducting component strongly influences the $T_c$. BEDT-TTF is an example of a fairly flexible donor molecule which has provided a variety of the cation radical salts. With various kinds of inorganic anions, BEDT-TTF has produced many ambient-pressure superconductors. Other conducting component molecules of the organic superconductors presently known are TMTSF, BEDO-TTF, DMET, MDT-TTF, and M(dmit)$_2$ (M = Ni, Pd).[2,3] Recent investigations involving $C_{60}$ salts expand the field to include molecular superconductors.[4] This work has brought an abrupt rise of the $T_c$ to more than 30 K.

As a planar donor molecule, BEDT-TTF has the highest recorded $T_c$'s in the cation radical salt κ-(BEDT-TTF)$_2$Cu[N(CN)$_2$]X ($T_c$ = 12.8 K at 0.3 kbar for X = Cl; $T_c$ = 11.8 K at ambient pressure for X = Br).[5,6] Compared to the crystal structures of other molecular superconductors, this donor presents the richest variety of packing patterns. The linear relationship between $T_c$ and effective volume ($V_{eff}$) has been determined using the unit cell volume ($V_{cell}$), anion volume ($V_a$), and the numbers of conduction electrons ($n$) in the unit cell:[1,7]

$$V_{eff} = (V_{cell} - V_a)/n$$

However, factors that influence the donor packing motif have not been explicitly examined.

Recently, we prepared two ambient-pressure BEDT-TTF superconductors, κ-(BEDT-TTF)$_2$Cu(CN)[N(CN)$_2$] and κ-(BEDT-TTF)$_2$Cu$_2$(CN)$_3$.[8] In subsequent works,[9] we proposed that the planar anion layers having a particular pattern of anion openings allow BEDT-TTF to construct the κ-type salt. The anion opening was defined as the space which was not occupied by the anion atoms in the anion layer. Detailed analyses of the crystal structures of BEDT-TTF superconductors having the planar anion layers revealed that the cores of the anion openings correlate with specific positions of the donor hydrogen atoms which are closest to the anion layer within each ethylene group. The pattern of the cores exhibits a 1:1 correspondence with the donor packing motif.

This paper reports the conducting properties and a full description of the crystal structures of the superconductors κ-(BEDT-TTF)$_2$Cu(CN)[N(CN)$_2$] and κ-(BEDT-TTF)$_2$Cu$_2$(CN)$_3$. The geometry of the cores of the anion openings and an improved definition of the space in which the conduction carrier can delocalize effectively are discussed. We show that this volume has a strong correlation with $T_c$.

For conciseness, we have abbreviated BEDT-TTF as ET to represent chemical formulas of salts, e.g. κ-(BEDT-TTF)$_2$Cu(CN)[N(CN)$_2$] is referred as κ-(ET)$_2$Cu(CN)[N(CN)$_2$]. Furthermore, we have found a significant difference in the conducting properties of κ-(ET)$_2$Cu$_2$(CN)$_3$ compared to what has been previously reported,[10-12] although the unit cell parameters and packing motif are in agreement. Because of the difference in conducting properties, we refer to our salt as κ′-(ET)$_2$Cu$_2$(CN)$_3$.

† Kyoto University.
‡ Institute for Molecular Science.
§ Institute for Protein Research, Osaka University.
* Abstract published in *Advance ACS Abstracts*, October 15, 1993.

(1) Saito, G. *Phosphorus Sulfur* **1992**, *67*, 345.
(2) Williams, J. M.; Ferraro, J. R.; Thorn, R. J.; Carlson, K. D.; Geiser, U.; Wang, H. H.; Kini, A. M.; Whangbo, M.-H. *Organic Superconductors (Including Fullerenes): Synthesis, Structure, Properties, and Theory*; Prentice Hall: Englewood Cliffs, NJ, 1992.
(3) Saito, G. In *New Materials*, Joshi, S. K., Tsuruta, T., Rao, C. N. R., Nagakura, S., Eds.; Narosa Publishing House: New Delhi, India, 1992; p 127.
(4) Haddon, R. C. *Acc. Chem. Res.* **1992**, *25*, 127.
(5) Kini, A. M.; Geiser, U.; Wang, H. H.; Karlson, K. D.; Williams, J. M.; Kwok, W. K.; Vandervoort, K. G.; Thompson, J. E.; Stupka, D. L.; Jung, D.; Whangbo, M.-H. *Inorg. Chem.* **1990**, *29*, 2555.
(6) Williams, J. M.; Kini, A. M.; Wang, H. H.; Karlson, K. D.; Geiser, U.; Montgomery, L. K.; Pyrka, G. J.; Watkins, D. M.; Kommers, J. M.; Boryschuk, S. J.; Crouch, A. V. S.; Kowck, W. K.; Schirber, J. E.; Overymyer, D. L.; Jung, D.; Whangbo, M.-H. *Inorg. Chem.* **1990**, *29*, 3272.
(7) Saito, G.; Urayama, H.; Yamochi, H.; Oshima, K. *Synth. Met.* **1988**, *27*, A331.
(8) Komatsu, T.; Nakamura, T.; Matsukawa, N.; Yamochi, H.; Saito, G.; Ito, H.; Ishiguro, T.; Kusunoki, M.; Sakaguchi, K. *Solid State Commun.* **1991**, *80*, 843.
(9) Yamochi, H.; Nakamura, T.; Komatsu, T.; Matsukawa, N.; Inoue, T.; Saito, G.; Mori, T.; Kusunoki, M.; Sakaguchi, K. *Solid State Commun.* **1992**, *82*, 101. Yamochi, H.; Komatsu, T.; Saito, G.; Kusunoki M.; Sakaguchi, K. *Synth. Met.* **1993**, *56*, 2207.
(10) Geiser, U.; Wang, H. H.; Carlson, K. D.; Williams, J. M.; Charlier, H. A., Jr.; Heindl, J. E.; Yaconi, J. A.; Love, B. J.; Lathrop, M. W.; Schirber, J. E.; Overmyer, D. L.; Ren, J.; Wangbo, M.-H. *Inorg. Chem.* **1991**, *30*, 2586.
(11) Bu, X.; Frost-Jensen, A.; Allendoerfer, R.; Lederle, B.; Naughton, M. J. *Solid State Commun.* **1991**, *79*, 1053.
(12) Papavassiliou, G. C.; Lagouvardos, D. J.; Kakoussis, V. C.; Terzis, A.; Hountas, A.; Hilti, B.; Mayer, C.; Zambounis, J. S.; Pfeiffer, J.; Whangbo, M.-H.; Ren, J.; Kang, D. B. *Mater. Res. Symp. Proc.* **1992**, *247*, 535.

0002-7863/93/1515-11319$04.00/0 

## Experimental Section

**Preparation of the Superconductors.** Both $\kappa$-$(ET)_2Cu(CN)[N(CN)_2]$ and $\kappa'$-$(ET)_2Cu_2(CN)_3$ were prepared by the electrocrystallization of BEDT-TTF in the presence of $Cu^+$, $CN^-$, and $N(CN)_2^-$ under a constant current of 0.5–2 $\mu$A.[8] Combinations of (1) tetraphenylphosphonium dicyanamide ($Ph_4PN(CN)_2$) and copper(I) cyanide (CuCN), (2) sodium dicyanamide ($NaN(CN)_2$), CuCN, and 18-crown 6-ether, and (3) copper(I) dicyanamide ($CuN(CN)_2$), potassium cyanide (KCN), and 18-crown 6-ether were employed as the supporting electrolytes. The solvents used were (a) benzonitrile (PhCN), (b) PhCN + ca. 10 vol % ethanol (EtOH), (c) 1,1,2-trichloroethane (TCE) + ca. 10 vol % EtOH, or (d) PhCN + ca. 20 vol % TCE + 2 vol % EtOH.

Electrolyte **2** in solvent **c** or electrolyte **3** in any solvent gave the needle-shaped semiconductor, $\theta$-$(ET)_2Cu_2(CN)[N(CN)_2]_2$.[13] Typical preparation procedures of the superconductors are described below.

$\kappa$-$(ET)_2Cu(CN)[N(CN)_2]$. Using an H-shaped glass cell with a glass frit separating two chambers, 9.0 mg of BEDT-TTF, 40.8 mg of $Ph_4PN(CN)_2$, and 15.1 mg of CuCN were suspended in a mixture of PhCN (16 mL) and EtOH (2 mL). After all undissolved materials sedimented, a constant current of 0.5 $\mu$A was applied to the supernatant using platinum electrodes (the diameter of anode was 2 mm). All the above processes were carried out under a nitrogen atmosphere. After a 1-week period, black rhombus and/or rectangular plates with metallic luster were collected on a glass filter, washed with methanol, and dried in vacuo. A typical dimension of the crystal was 1.7 mm × 0.6 mm × 0.01–0.02 mm. The most developed face and its longitudinal direction corresponded to the crystallographic *bc*-plane and *b*-axis, respectively.

$\kappa'$-$(ET)_2Cu_2(CN)_3$. The preparation of this salt was similar to that of $\kappa$-$(ET)_2Cu(CN)[N(CN)_2]$. The combination of electrolyte **2** in solvent **a** or **d** gave single crystals of $\kappa'$-$(ET)_2Cu_2(CN)_3$ as black rhombus plates along with crystals of $\kappa$-$(ET)_2Cu(CN)[N(CN)_2]$ having poor quality. $\kappa'$-$(ET)_2Cu_2(CN)_3$ crystals were typically 1.1 mm × 1.2 mm × 0.02 mm. The diagonals of the most developed face corresponded to the *b*- and *c*-axes, respectively.

The reagents and the solvents for the electrocrystallization were prepared as follows: $Ph_4PN(CN)_2$ was prepared[14] and recrystallized from EtOH or from a mixture of EtOH and water. CuCN was washed with diluted $H_2SO_4$ to eliminate $Cu^{2+}$. 18-Crown 6-ether was recrystallized from acetonitrile. Commercially available $NaN(CN)_2$ (Aldrich) was recrystallized from EtOH. $CuN(CN)_2$ was prepared according to the reported procedure.[15] KCN was recrystallized from a mixture of water and EtOH. All of the solvents for the electrocrystallization were treated and stored under a nitrogen atmosphere. PhCN was washed with hydrochloric acid, dried over potassium carbonate, vacuum distilled from phosphorus pentaoxide, and distilled from potassium carbonate in vacuo. EtOH was distilled from magnesium ethoxide. TCE was washed with $H_2SO_4$, dried over calcium chloride, and distilled. Just before its use, this solvent was passed through the column packed with the alumina (ICN Biomedicals, ICN Alumina B-Super I).

**Crystal Structure Analysis.** X-ray data were collected using the graphite-monochromated Mo K$\alpha$ radiation using the $\omega$-scan technique. Together with the observed densities, full-matrix least-squares refinements of the models obtained by direct methods gave the compositions and the structures of the salts.[16] Anisotropic thermal parameters were adopted for all non-hydrogen atoms. Hydrogen atoms were not included in the refinements and the calculation of the *R*-values. Table I summarizes the crystal data. The detailed procedures of the analyses are described in previous reports,[9] in which the orientations of the CN groups were determined mainly on the basis of the temperature factors.

Conductivity measurements were performed before the crystals were identified with X-ray measurements in order that radiation damage would not affect the results. Unit cell parameters and diffraction patterns of the (*h*,0,0), (0,*k*,0), and (0,0,*l*) reflections were used for identification purposes.

## Results

**Conducting Properties of $\kappa$-$(ET)_2Cu(CN)[N(CN)_2]$ and $\kappa'$-$(ET)_2Cu_2(CN)_3$.** Figure 1 shows the temperature dependences of the resistivity of $\kappa$-$(ET)_2Cu(CN)[N(CN)_2]$ and $\kappa'$-$(ET)_2Cu_2(CN)_3$.[8] The conductivities and the $T_c$'s of these $\kappa$-type salts are summarized in Table II.

It is noteworthy that both of these salts exhibit a monotonical decrease of the resistivity with temperature above the $T_c$'s. This behavior is in sharp contrast to those of the other 10 K class ambient-pressure BEDT-TTF superconductors of $\kappa$-$(ET)_2Cu(NCS)_2$ and $\kappa$-$(ET)_2Cu[N(CN)_2]Br$. The latter show semiconductive behavior with the resistivity maximum around 90 K.[1-3]

For $\kappa$-$(ET)_2Cu(CN)[N(CN)_2]$, the anisotropy of the conductivity between parallel and perpendicular directions to the *bc*-plane at room temperature was 230:1. The magnitude of the anisotropy is intermediate between that of $\kappa$-$(ET)_2Cu(NCS)_2$ (600:1) and of $\kappa$-$(ET)_2Cu[N(CN)_2]Br$ (200:1).[8] The magnitude of anisotropy corresponds to the inter-donor-layer shortest sulfur to sulfur (S···S) distance (see Table IV).

**Table I.** Crystal, Data Collection, and Refinement Parameters for $\kappa$-$(ET)_2Cu(CN)[N(CN)_2]$ and for $\kappa'$-$(ET)_2Cu_2(CN)_3$

| | $\kappa$-$(ET)_2Cu(CN)[N(CN)_2]$ | $\kappa'$-$(ET)_2Cu_2(CN)_3$ |
|---|---|---|
| space group | monoclinic, $P2_1$ | monoclinic, $P2_1/c$ |
| unit cell parems | | |
| *a*, Å | 16.00(1) | 16.113(5) |
| *b*, Å | 8.631(4) | 8.560(3) |
| *c*, Å | 12.90(3) | 13.331(6) |
| $\beta$, deg | 110.97(8) | 112.94(3) |
| *V*, Å$^3$ | 1663(4) | 1693(1) |
| *Z* | 2 | 2 |
| no. obsd reflcns ($F_o > n\sigma(F_o)$)[a] | 4390 ($n$ = 0), 2504 ($n$ = 4) | 3678 ($n$ = 0), 1431 ($n$ = 4.5) |
| no. refined variables | 396 | 205 |
| $2\theta_{max}$, deg | 45 | 45 |
| final *R*-value,[b] % | 5.06 | 12.10 |
| density, g cm$^{-3}$: obsd; calcd | $1.85_8$; 1.846 | $1.89_2$; 1.911 |

[a] For refinements and calculations of *R*-values, the reflections of which $F_o > n\sigma(F_o)$ were taken into account ($n$ = 4 for the $Cu(CN)[N(CN)_2]$ salt; $n$ = 4.5 for the $Cu_2(CN)_3$ salt). [b] $R = (\Sigma||F_o| - |F_c||)/\Sigma|F_o|$.

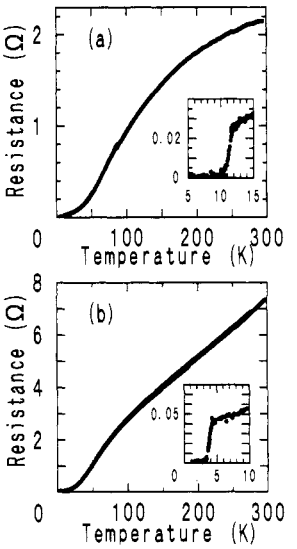


**Figure 1.** Temperature dependence of the resistivity of (a) $\kappa$-$(ET)_2Cu(CN)[N(CN)_2]$ and (b) $\kappa'$-$(ET)_2Cu_2(CN)_3$ in the *bc*-planes.

**Table II.** Summary of the Conducting Properties of $\kappa$-$(ET)_2Cu(CN)[N(CN)_2]$ and $\kappa'$-$(ET)_2Cu_2(CN)_3$

| | $\sigma_{rt}$,[a] S cm$^{-1}$ | $\sigma_{max}$,[b] S cm$^{-1}$ | $T_c$,[c] K |
|---|---|---|---|
| $\kappa$-$(ET)_2Cu(CN)[N(CN)_2]$ | 12–50 | 1100–1800 | 11.2 |
| $\kappa'$-$(ET)_2Cu_2(CN)_3$ | 10–33 | 610–1300 | 3.8 |

[a] Conductivity at room temperature in the *bc*-plane. [b] Conductivity at the onset temperature of the superconducting transition in the *bc*-plane. [c] Superconducting transition temperature defined as the midpoint of the resistivity jump.

(13) Komatsu, T.; et al. Manuscript in preparation.
(14) Köhler, V. H.; Lischiko, T. P.; Hartung, H.; Golub, A. M. *Z. Anorg. Allg. Chem.* **1974**, *403*, 35.
(15) Keller, R. N.; Wycoff, H. D. *Inorg. Synth.* **1946**, *2*, 1.
(16) The programs used in the analyses are SHELX76 and SHELX86 by G. Sheldrick.

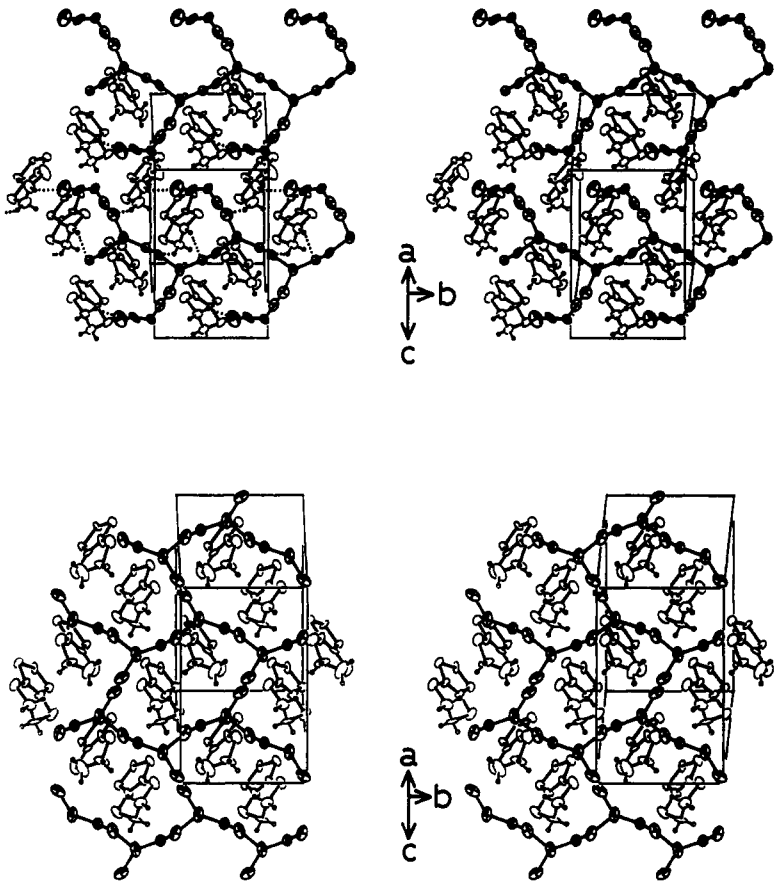


**Figure 2.** Stereoviews of the crystal structures of $\kappa$-$(ET)_2Cu(CN)[N(CN)_2]$ (top) and $\kappa'$-$(ET)_2Cu_2(CN)_3$ (bottom). Viewpoints are projected onto the *bc*-plane. Only half-sections of the donor molecules were drawn to simplify the figures. In the case of the $\kappa$-$(ET)_2Cu(CN)[N(CN)_2]$, the dotted lines indicate the significant atomic contacts between the donor hydrogen atoms and the anion atoms.

Previously, we examined the effect of isotopic substitution for $\kappa$-$(ET)_2Cu(CN)[N(CN)_2]$. Deuterium substitution of the ethylene hydrogen atoms of BEDT-TTF molecules does not alter the unit cell parameters at room temperature.[17] Thus, $\kappa$-$(ET\text{-}d_8)_2Cu(CN)[N(CN)_2]$ must be isostructural to the original salt. Also, in the metallic region, both the isotopically substituted salt and the unsubstituted salt exhibit the same temperature dependence of the resistivity. However, $\kappa$-$(ET\text{-}d_8)_2Cu(CN)[N(CN)_2]$ shows the increased $T_c$ of 12.3 K, which is the highest value among the ambient-pressure BEDT-TTF superconductors at present.[18]

**Crystal Structures of $\kappa$-$(ET)_2Cu(CN)[N(CN)_2]$ and $\kappa'$-$(ET)_2Cu_2(CN)_3$.** The crystal structure analyses of the superconductors $\kappa$-$(ET)_2Cu(CN)[N(CN)_2]$ and $\kappa'$-$(ET)_2Cu_2(CN)_3$ show that the donor molecules form typical $\kappa$-type conducting layers in both salts.[9] The donor forms a face-to-face dimer which assembles orthogonally to adjacent dimers. A two-dimensional sheet parallel to the crystallographic *bc*-plane is formed.

In the case of $\kappa$-$(ET)_2Cu(CN)[N(CN)_2]$, two crystallographically independent donor molecules form the dimer with an interplanar distance of 3.7 Å and a dihedral angle of 2.1° (Figure 2). In the BEDT-TTF dimer, one molecule has an eclipsed conformation of the ethylene groups and the other has a staggered conformation without any indications of disorders. This fact suggests that semiconductive behaviors of other 10 K class BEDT-TTF superconductors mentioned above are correlated to the disorder of the ethylene groups.[19]

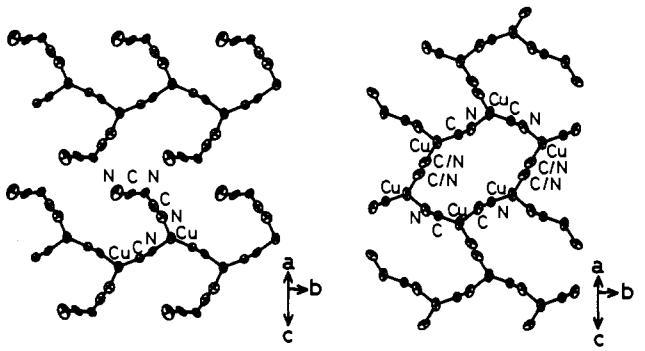


**Figure 3.** Anion layer of $\kappa$-$(ET)_2Cu(CN)[N(CN)_2]$ (left) and $\kappa'$-$(ET)_2Cu_2(CN)_3$ (right). Viewpoints are projected onto the *bc*-plane.

Intermolecular S··S contacts between donor molecules that are shorter than the sum of van der Waals radii (vdW = 1.80 Å) are observed in this salt and exist only between the dimers similar to $\kappa$-$(ET)_2Cu[N(CN)_2]Br$.[9] The anion layer contains an infinite chain of -(Cu–C–N)- atoms along the *b*-axis (Figure 3). Dicyanamide anion coordinates with the copper atom as a pendant with a terminal nitrogen atom. Between the anion chains, atomic contacts shorter than the sum of vdW were not observed. This feature is also observed for the structure of $\kappa$-$(ET)_2Cu(NCS)_2$.[20] The dihedral angle between the donor best plane and the anion

(17) For the two crystals of the deuterium-substituted salt of $\kappa$-$(ET)_2Cu(CN)[N(CN)_2]$, the unit cell parameters ($a$ (Å), $b$ (Å), $c$ (Å), $\beta$ (deg), $V$ (Å$^3$)) are 16.019(7), 8.597(4), 12.976(5), 111.31(3), 1665(1) and 15.984(3), 8.622(2), 12,898(4), 110.89(2), 1660.0(8). Also, the ($h$,0,0), (0,$k$,0), and (0,0,$l$) diffraction patterns of these crystals were identical to those of the unsubstituted ones.

(18) Saito, G.; Yamochi, H.; Nakamura, T.; Komatsu, T.; Matsukawa, N.; Inoue, T.; Ito, H.; Ishiguro, T.; Kusunoki, M.; Sakaguchi, K. *Synth. Met.* **1993**, *56*, 2883.

(19) Presently proposed mechanisms for the semiconductive behaviors of the 10 K class of BEDT-TTF superconductors are summarized in: Pouget, J. P. *Mol. Cryst. Liq. Cryst.* **1993**, *230*, 101.

(20) Urayama, H.; Yamochi, H.; Saito, G.; Nozawa, K.; Sugano, T.; Kinoshita, M.; Sato, S.; Oshima, K.; Kawamoto, A.; Tanaka, J. *Chem. Lett.* **1988**, 55.

Table III. Summary of the Calculated Band Structures of κ-(ET)$_2$Cu(CN)[N(CN)$_2$] and κ'-(ET)$_2$Cu$_2$(CN)$_3$ with the Results for κ-(ET)$_2$Cu(NCS)$_2$ Also Listed for Comparison

| | tot. bandwidth of four HOMO bands, eV | tot. bandwidth of upper two HOMO bands, eV | $N(\epsilon_F)$,[a] states·eV$^{-1}$·molecule$^{-1}$·spin$^{-1}$ | cross section of Fermi surface around Z point, % of the first Brillouin zone |
|---|---|---|---|---|
| κ-(ET)$_2$Cu(CN)[N(CN)$_2$] | 1.03 | 0.52 | 0.99 | 18 |
| κ'-(ET)$_2$Cu$_2$(CN)$_3$ | 1.00 | 0.49 | 1.04 | 21 |
| κ-(ET)$_2$Cu(NCS)$_2$ | 1.15 | 0.54 | 0.90 | 18 |

[a] The density of states at the Fermi level. It should be noted that the values are given in the units of a single BEDT-TTF molecule rather than a formula unit of (BEDT-TTF)$_2$X.

plane is ca. 70°. Atomic contacts between the donor hydrogen atoms and the anion atoms are formed by using both parts of the infinite chain and the pendant of the anion.[21]

The unit cell parameters and the packing motif of κ'-(ET)$_2$Cu$_2$(CN)$_3$ are substantially similar to that of κ-(ET)$_2$Cu$_2$(CN)$_3$ reported by Geiser et al.[10] and Bu et al.[11] Both groups claim the complex has a semiconductive nature at ambient pressure. Contrary to these results, we observe the superconducting transition at 2.0–3.8 K without any semiconductive behavior below room temperature at ambient pressure. Previously, Papavassiliou et al. reported κ-(ET)$_2$Cu$_2$(CN)$_3$ without semiconductive behavior having a similar composition and crystal structure.[12] The differences of the transport properties of these salts may arise from the slight differences of the crystal structures together with the crystal qualities. However, inaccuracies in the structural analyses inhibit us from a detailed comparison of the results.

In κ'-(ET)$_2$Cu$_2$(CN)$_3$, one BEDT-TTF molecule is crystallographically unique and has a planar π-system ($C_6S_8$ skeleton). The ethylene groups form a staggered conformation. In the dimer, two donor molecules are related by an inversion center and show a bond-over-ring overlap with an interplanar distance of 3.7 Å (Figure 2). Similar to κ-(ET)$_2$Cu(CN)[N(CN)$_2$], intermolecular S··S contacts shorter than the sum of vdW were observed only between dimers. The anion layer is composed of the two-dimensional network of coppers and cyano groups (Figure 3). Among anion atoms, only the ordered cyano groups form atomic contacts with donor hydrogen atoms, and they are rather weak.[21]

**Band Electronic Structures of κ-(ET)$_2$Cu(CN)[N(CN)$_2$] and κ'-(ET)$_2$Cu$_2$(CN)$_3$.** The intermolecular overlap integrals ($S$) in these κ-type salts were obtained by applying the simple extended Hückel method[22] on the basis of the donor layer structures at room temperature. With the assumption of the proportionality between the transfer integral ($t$) and $S$ as $t = ES$ ($E$ = −10 eV), the tight-binding approximation gives the dispersion relation, the Fermi surfaces, and the density of state (DOS) as shown in Figure 4 and Table III. In both cases, the four highest occupied molecular orbitals (HOMO's) were taken into account to evaluate the band electronic structure near the Fermi surface, since the unit cell contains the four donor molecules. Since ESR measurements showed no evidence for the existence of $Cu^{2+}$ ion in both salts, the formal charges of the donor molecules are estimated as +0.5. Although two BEDT-TTF molecules are crystallographically independent in κ-(ET)$_2$Cu(CN)[N(CN)$_2$], judging from the intramolecular bond lengths, the donor molecules are of the same charge.

Figure 4 shows that the Fermi surfaces of κ-(ET)$_2$Cu(CN)[N(CN)$_2$] consist of two surfaces, a closed and an open one with

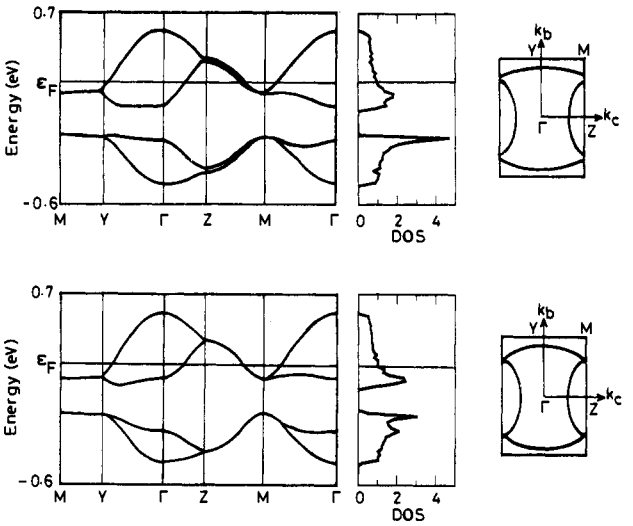


Figure 4. Dispersion relation, density of state (DOS in states·eV$^{-1}$·molecule$^{-1}$·spin$^{-1}$), and Fermi surfaces (left to right) of κ-(ET)$_2$Cu(CN)[N(CN)$_2$] (top) and κ'-(ET)$_2$Cu$_2$(CN)$_3$ (bottom) calculated by the tight-binding method based on the extended Hückel approximation. The Fermi levels are indicated as $\epsilon_F$.

a gap of 14 meV on the $ZM$ line. The calculated band structure is in accordance with the sign of the observed thermoelectric power. The sign is negative along the $b$-axis and positive along the $c$-axis from room temperature to slightly above $T_c$ (ca. −20 and +8 μV/K at room temperature, respectively).[18] The band structure is very similar to that of κ-(ET)$_2$Cu(NCS)$_2$, which shows the Shubnikov–de Haas oscillations below 1 K and above 8 T.[23]

The band structure of κ'-(ET)$_2$Cu$_2$(CN)$_3$ resembles that of κ-(ET)$_2$Cu(CN)[N(CN)$_2$]. However, the Fermi surfaces are degenerate on the $ZM$ line because of the requirement of the space group. This band structure is similar to that of κ-(ET)$_2$I$_3$[24] rather than of κ-(ET)$_2$Cu(NCS)$_2$.

Investigations of the transport properties under the magnetic field on these κ-type salts are in progress.[25]

## Discussion

**Factors Which Determine the Donor Packing Motif.** As is mentioned in the Introduction, BEDT-TTF can give various modifications of salts even with the same anion species.[1,2] This fact suggests that the packing behavior of this donor in its cation radical salt is subordinate to the structure of the counter components in the salt. The ethylene groups of BEDT-TTF are situated at the crystallographic border with the anion layer. In order to uncover the relationship between the structure of the counter component and the donor packing motif, the relative orientation of the alkyl groups to the anion layer must be inspected.

Since the donor–anion atomic contacts have been regarded to play a crucial role in governing the packing pattern and

(21) Atomic contacts (Å) between donor hydrogen and anion atoms shorter than the sum of vdW are listed below. In parentheses after the names of the atoms, the symmetry operations are indicated which are used to obtain the actual coordinates from the atomic parameters in Tables S1 and S2 (see also Table S17). κ-(ET)$_2$Cu(CN)[N(CN)$_2$]: H12A(1 − $x$, $y$ − 0.5, −$z$)–N40($x$, $y$, $z$) = 2.67, H13B(1 − $x$, $y$ − 0.5, −$z$)–N41(−$x$, 0.5 + $y$, −$z$) = 2.56, H17B($x$, $y$, $x$)–N41($x$, 1 + $y$, $z$) = 2.58, H18B($x$, $y$, $z$)–N42($x$, $y$, $z$) = 2.51, H32B($x$, $y$, $z$)–C51($x$, $y$, $z$) = 2.77, H33B($x$, 1 + $y$, $z$)–N50(−$x$, 0.5 + $y$, 1 − $z$) = 2.61, H37A(1 − $x$, 0.5 + $y$, −$z$)–N50(−$x$, 0.5 + $y$, −$z$) = 2.66, H37A(1 − $x$, 0.5 + $y$, −$z$)–C51(−$x$, 0.5 + $y$, −$z$) = 2.81, H37B(1 − $x$, 0.5 + $y$, −$z$)–C44(−$x$, 0.5 + $y$, −$z$) = 2.88, H37B(1 − $x$, 0.5 + $y$, −$z$)–C43(−$x$, 0.5 + $y$, −$z$) = 2.89. κ'-(ET)$_2$Cu$_2$(CN)$_3$: H13B($x$, $y$, $z$)–N103(−$x$, $y$ − 0.5, −$z$) = 2.68, H17B(1 − $x$, −$y$, −$z$)–C101(−$x$, −$y$, −$z$) = 2.89.

(22) Mori, T.; Kobayashi, A.; Sasaki, Y.; Kobayashi, H.; Saito, G.; Inokuchi, H. *Bull. Chem. Soc. Jpn.* **1984**, *57*, 627.

(23) Oshima, K.; Mori, T.; Inokuchi, H.; Urayama, H.; Yamochi, H.; Saito, G. *Phys. Rev.* **1988**, *B38*, 938.

(24) Kobayashi, A.; Kato, B.; Kobayashi, H.; Moriyama, S.; Nishino, Y.; Kajita, K.; Sasaki, W. *Chem. Lett.* **1987**, 459. The atomic parameters were taken from a private communication from Dr. A. Kobayashi (1992).

(25) Nakamura, T.; Komatsu, T.; Saito, G.; Osada, T.; Kagoshima, S.; Miura, N.; Kato, K.; Maruyama, Y.; Oshima, K. *J. Phys. Soc. Jpn*, in press.

conformation of the donor molecule,[26] it is interesting to elucidate such intermolecular interactions.

In order not to overestimate the donor–anion atomic contacts (C–H···anion), the discussion concerns only the significant intermolecular atomic contacts which are shorter than (vdW − 0.11) Å.[27] Among the superconducting BEDT-TTF salts listed in Table IV, all of the $\beta$-type salts, $\kappa$-$(ET)_2I_3$, $\kappa'$-$(ET)_2Cu_2(CN)_3$, and $\kappa$-$(ET)_2Cu[N(CN)_2]Br$ show no significant donor–anion atomic contacts. In other salts, a variety of such contacts are observed. In the case of $\alpha$-type salts, three BEDT-TTF molecules are crystallographically independent. Among them, two of the donor molecules exhibit significant donor–anion atomic contacts with anion atoms by using both ethylene groups in each molecule. In $\kappa$-$(ET)_2Cu(NCS)_2$, such atomic contacts are found only between an ethylene hydrogen atom and the anion sulfur atom in the infinite chain of ~(Cu–N–C–S)~. Conversely, the anion atoms in the infinite chain of ~(M–C–N)~ (M = Ag, Cu) and in other positions give significant atomic contacts in $\kappa$-$(ET)_2Ag(CN)_2{\cdot}H_2O$ and $\kappa$-$(ET)_2Cu(CN)[N(CN)_2]$.[28]

On the basis of the above results, it is difficult to conclude that the donor–anion atomic contacts solely determine the donor packing motif.

Despite the difference in the anion structure and the patterns of donor–anion contacts, when viewing along the direction perpendicular to the anion layer, $\kappa$-$(ET)_2Cu(CN)[N(CN)_2]$ and $\kappa'$-$(ET)_2Cu_2(CN)_3$ contain ethylene groups located at anion openings (see Figure 2). The existence of such anion openings was originally noticed only for $\kappa$-$(ET)_2Cu[N(CN)_2]X$ (X = Br, Cl). The pattern for all of the salts has not been characterized.[29]

Since donor molecules or dimers fit into the openings, to construct the crystal, the shape and the size of the anion openings are the decisive factors of the donor stacking pattern. Consequently, the openings govern the dispersion relation of the band electronic structure in the two-dimensional (2D) plane. Also the openings function as pathways of the tunnel coupling between the 2D conducting layers. Hence, the size of the openings, the thickness of the anion layer, and the short atomic contacts between the neighboring donor layers through the openings are important factors to having a greater three-dimensional electronic structure.[18,25]

In the previous reports,[9] we had proposed that the planar anion layers having a generalized pattern of openings form $\kappa$-type BEDT-TTF salts. Figure 5a illustrates this pattern which can be likened

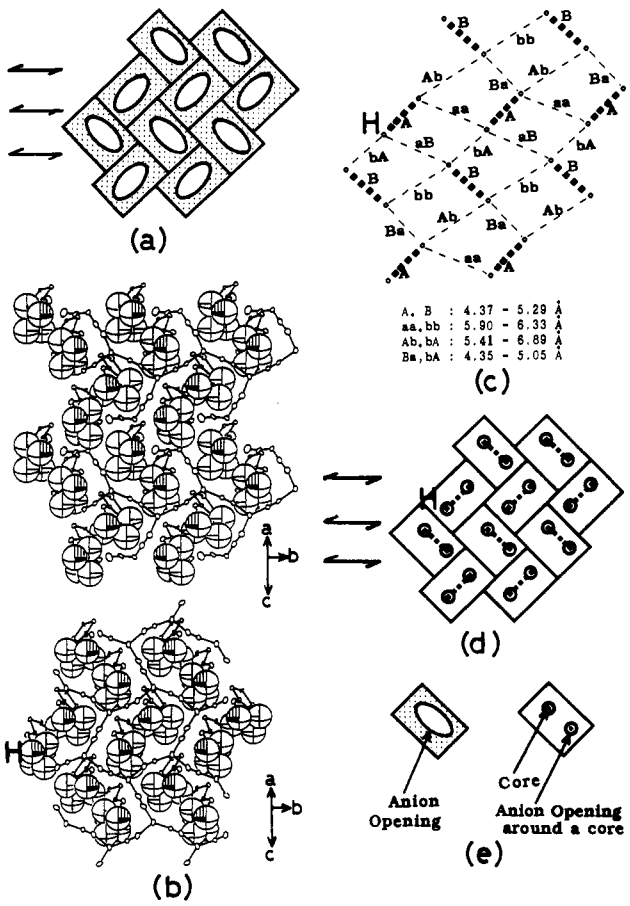


**Figure 5.** Crystal structure and pattern of openings of the $\kappa$-type BEDT-TTF salts. The anion layer projections of the crystal structures are illustrated for $\kappa$-$(ET)_2Cu(CN)[N(CN)_2]$ (top in (b)) and $\kappa'$-$(ET)_2Cu_2(CN)_3$ (bottom in (b)). In (a), an ellipse indicates an opening which holds a pair of hydrogen atoms and the anion is located in the shaed region. In (a) and (d), the arrows indicate the (pseudo-) 2-fold screw axes. In (c) and (d), the thick dotted line links two hydrogen atoms within a donor dimer. A dotted line forms an angle of 85–90° with the one related by the (pseudo-) screw operation. (e) shows the relationship between an "anion opening" and "anion openings around cores". See also footnote 30.

to the alternate leaves on a twig. Namely, the anion layers possess rectangular to elliptic openings which are related by the screw operation. The estimated area of each opening is around 19 Å$^2$, which is inside a rectangular unit of ca. 55 Å$^2$.

When the hydrogen atoms were drawn as the spheres with vdW of 1.2 Å, a common feature appears. Namely, two hydrogen atoms belonging to the donor dimer occupy an opening (Figure 5b). These hydrogen atoms are closest to the anion layer, and their positions determine the donor packing motif as is described below.

We define the "core" of the anion opening as the projected position of the donor hydrogen atom closest to the anion layer. In this paper, patterns of the cores are described to carry out a comparison of the pattern of the openings with those of different modifications having the planar anion layers, i.e. $\alpha$-, $\beta$-, $\theta$-, and $\kappa$-type salts (see Table IV).

In the case of the $\kappa$-type salts, the projected positions of the hydrogen atoms onto the anion layer show a distorted checker pattern as illustrated in Figure 5c. The thick dotted lines in the figure correspond to hydrogen pairs of the face-to-face donor dimers. For the $\kappa$-type salts having the $P2_1/c$ or *Pnma* symmetry, the pairs of A and B, aa and bb, Ba and bA, and Ab and aB in the figure are related by the 2-fold screw operation and are equivalent. The above pairs are crystallographically independent in the other $\kappa$-type salts whose space groups are $P2_1$. However,

(26) Whangbo, M.-H.; Jung, D.; Ren, J.; Evain, M.; Novoa, J. J.; Mota, F.; Alvarez, S.; Williams, J. M.; Beno, M. A.; Kini, A. M.; Wang, H. H.; Ferraro, J. R. In *The Physics and Chemistry of Organic Superconductors*; Springer Proceedings in Physics Vol. 51, Saito, G.; Kagoshima, S., Eds.; Springer-Verlag: Berlin, 1990; p 262 and the references cited therein.

(27) A list of significant donor hydrogen to anion contacts is given in the supplementary material (Table S17). Because of the inherent nature of the X-ray crystal structure analysis, the coordinates of the hydrogen atoms are poor in accuracy for the BEDT-TTF salts. In this paper, the discussion dealing with the ethylene hydrogen atoms of the donor molecules is based on the calculated positional parameters of them, assuming a C–H bond length of 1.0 Å and an $sp^3$ configuration of the ethylene carbon atom. It should be noted that the value of 0.11 Å does not have a firm physical significance. However, the value corresponds to half of the square root of 0.05, which is usually adopted as the initial value for the mean square shift of the atomic position due to the thermal vibration in the structural analysis. Also it is interesting to compare the value of 0.11 Å to the differences between the van der Waals radii and the ionic radii for the halogen atoms, which are 0.11 and 0.22 Å for bromine and iodine, respectively.

(28) These positions are shown in Figure 2 and in the supplementary material (Table S17).

(29) Williams, J. M.; Wang, H. H.; Carlson, K. D.; Kini, A. M.; Geiser, U.; Schultz, A. J.; Kwok, W. K.; Welp, U.; Crabtreee, G. W.; Fleshler, S.; Whangbo, M.-H.; Schirber, J. E. *Physica C* 1991, *185–189*, 355.

(30) The following caption is the same for Figures 5 and 7–9: In the anion layer projection of the crystal structure, only half-sections of the donor molecules were drawn. In (b), the hydrogen atoms are drawn as spheres with a 1.2-Å radius. Hydrogen atoms which are located closest to the anion layers are shaded. In (c), circles indicate the anion-layer-projected positions of the hydrogen atoms closest to the anion layer. The distances between the neighboring sites are listed. In (d), the cores of the anion openings correspond to the centers of the open circles. In (b)–(d), sites labeled with "H" correspond to the same hydrogen atom.

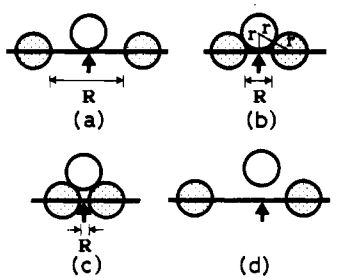


**Figure 6.** Illustration estimating the size of the open area around the core of the anion opening. Anion atoms are depicted as shaded circles, and ethylene hydrogen atoms are depicted as open circles. The thick line and the thick short arrow indicate the anion best plane and the position of the core of the anion opening, respectively. In every case, there are no donor–anion atomic contacts shorter than the sum of vdW. In (a) and (b), the hydrogen atom contacts with the anion best plane. Assuming the anion atoms have the same radius as that of a hydrogen atom ($r$ = 1.2 Å), the anion plane must have the open area with diameter ($R$) greater than $2(2r \cos 30° - r)$ = 1.76 Å. In (c) ($R$ < 1.76 Å), the hydrogen atom cannot gain contact with the anion best plane but can fit on a hollow site in the anion layer. (d) represents the usual case in the actual BEDT-TTF salt in which the anion best plane possesses a bigger opening than that depicted in (b), although the hydrogen atom closest to the anion layer does not gain contact with the anion best plane.

they are approximately related by the same operation in each group. Consequently, all of the $\kappa$-type salts exhibit the same pattern of cores of the anion openings as illustrated in Figure 5d.

The size of the open area around the core depends on the structure of the anion layer. In Figures 5 and 7–9, the anion opening around the core is represented as an open circle having a diameter of about 1.76 Å. The reason for this value is discussed below. The core of the anion opening corresponds to the center of the circle.

Simple arithmetic can estimate the size of the unoccupied area in the anion best plane. For example, we consider the case in which the ethylene hydrogen atom contacts with the anion best plane and exhibits no atomic contacts shorter than the sum of vdW with anion atoms (Figure 6a). Assuming that the radii of the anion atoms are the same as that of a hydrogen atom, a vacant area having a diameter ($R$) bigger than 1.76 Å is needed in the anion best plane (see Figure 6b). However, in some cases, the hollow sites can fit on the donor hydrogen atoms and $R$ is less than 1.76 Å (Figure 6c).

Figures 7–9 illustrate the anion layer projections of the crystal structures and the patterns of the cores of the anion openings for $\alpha$-,[31] $\beta$-,[32] and $\theta$-$(ET)_2I_3$[33] salts, respectively. Again, the ethylene groups are positioned at the openings of the anion layers and the hydrogen atoms occupy the openings.

Although $\alpha$-$(ET)_2I_3$ is not a superconducting salt, the donor packing motif is similar to that of the ambient-pressure superconductors $\alpha$-$(ET)_2MHg(SCN)_4$ (M = $NH_4$,[34] K[35]), which contain a thick anion layer of the triple-sheet structure.[36] The anion layers of these $\alpha$-type salts exhibit an identical pattern of cores at the openings. As illustrated in Figure 7c, these layers

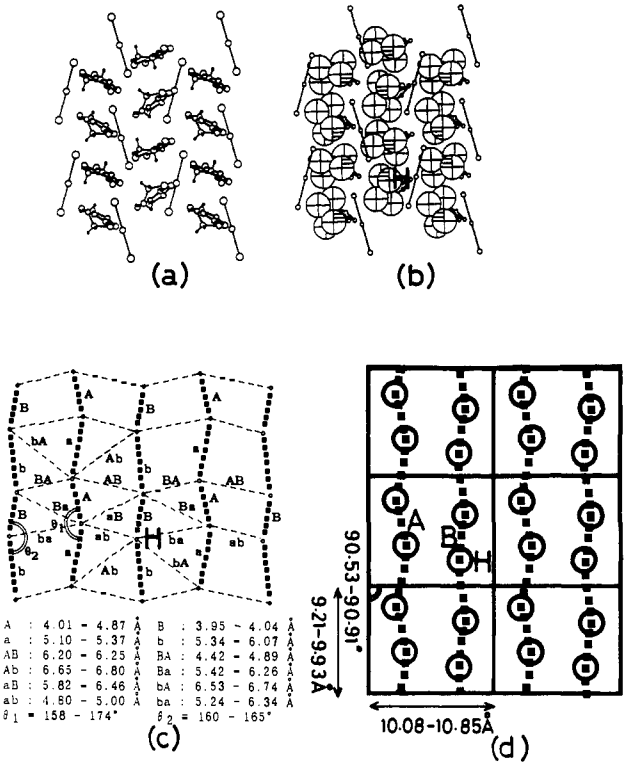


**Figure 7.** Crystal structure and pattern of the openings of the $\alpha$-type BEDT-TTF salts. The anion layer projections of the crystal structures for $\alpha$-$(ET)_2I_3$ are shown in (a) and (b). In (c) and (d), the thick dotted lines A and B correspond to the columnar stack of the donor molecules on the general position and at the center of inversion, respectively. See also footnote 30.

have a distorted checker pattern similar to that of the $\kappa$-type salt. However, the pattern for $\alpha$-type salts does not exhibit translational symmetry along the diagonal of the checker (for the $\kappa$-type salts, see the arrangement of dotted lines labeled "A" and/or "B" in Figure 5c). Also, the 2-fold screw operation does not exist for the $\alpha$-type salt. The anion plane in the crystallographic unit cell corresponds to the repetition unit of the pattern of the cores of the anion openings ($ab$- and $ac$-planes for $\alpha$-$(ET)_2I_3$ and $\alpha$-$(ET)_2MHg(SCN)_4$, respectively).

When the anion plane units are stacked, the pattern of the cores is represented as a zigzag alignment along the columnar direction of the donor stack (Figure 7d). Inevitably, the anion atoms are not located at the cores in $\alpha$-$(ET)_2I_3$. Conversely, in $\alpha$-$(ET)_2MHg(SCN)_4$, some of the anion atoms seem to position themselves close to the cores (Figure 10). However, in this situation, the hollow sites in the thick anion layer act as the anion openings to preserve the packing motif.

In $\beta$-type salts, the donor packing motives give two kinds of hydrogen atoms which are situated closest to the anion layer among each ethylene group. The distances between the anion layers and these hydrogen atoms differ from one another by more than 1.0 Å. This configuration is different from those of the other salts discussed in this paper. For the $\alpha$-, $\theta$-, and $\kappa$-type salts, the maximum differences of the distances between the hydrogen atoms of interest and the anion layers are less than 0.2 Å. For the $\beta$-type salts, the unoccupied areas around cores of the anion openings are indicated as big and small circles corresponding to hydrogen atoms which are situated closer and further to the anion layer in Figure 8d. The repetition unit of the pattern reveals the rectangle of ca. 6.1 Å × 9.1 Å.

As a $\theta$-type salt having the planar anion layer, only the $I_3$ salt has been reported.[33] Because of the symmetry of the crystal structure, one core of the anion opening is included in a rectangular unit of 5.04 Å × 4.96 Å (Figure 9).

(31) The atomic parameters were taken from: Bender, K.; Henning, I.; Schweitzer, D.; Dietz, K.; Endres, H.; Keller, H. J. *Mol. Cryst. Liq. Cryst.* **1984**, *108*, 359.

(32) The atomic parameters were taken from: Mori, T.; Kobayashi, A.; Sasaki, Y.; Kobayashi, H.; Saito, G.; Inokuchi, H. *Chem. Lett.* **1984**, 957.

(33) Kobayashi, A.; Kato, R.; Kobayashi, H.; Moriyama, S.; Nishino, Y.; Kajita, K.; Sasaki, W. *Chem. Lett.* **1986**, 2017. Kobayashi, H.; Kato, R.; Kobayashi, A.; Nishino, Y.; Kajita, K.; Sasaki, W. *Chem. Lett.* **1986**, 833. the atomic parameters were taken from a private communication from Dr. A. Kobayashi (1992).

(34) Wang, H. H.; Carlson, K. D.; Geiser, U.; Kwok, W. K.; Vashon, M. D.; Thompson, J. E.; Larsen, N. F.; McCabe, G. D.; Hulscher, R. S.; Williams, J. M. *Physica C* **1990**, *166*, 57.

(35) Its superconducting portion is thought to possess a fibrillike structure: Ito, H.; Kaneko, H.; Ishiguro, T.; Ishimoto, H.; Kono, K.; Horiuchi, S.; Komatsu, T.; Saito, G. *Solid State Commun.* **1993**, *85*, 1005.

(36) Mori, H.; Tanaka, S.; Oshima, M.; Saito, G.; Mori, T.; Maruyama, Y.; Inokuchi, H. *Bull. Chem. Soc. Jpn.* **1990**, *63*, 2183.

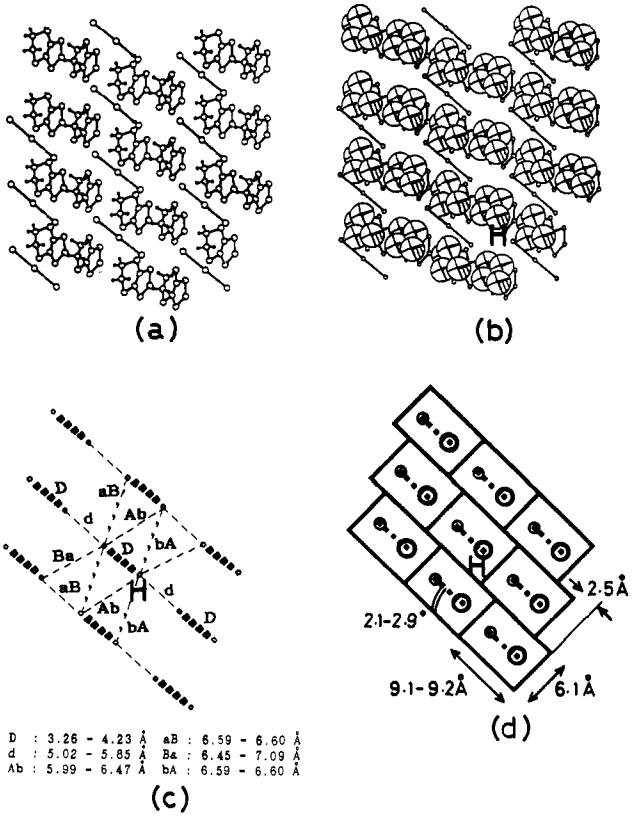


**Figure 8.** Crystal structure and pattern of the openings of the $\beta$-type BEDT-TTF salts. The anion layer projections of the crystal structures are illustrated for $\beta$-$(ET)_2I_3$ in (a) and (b). In (c) and (d), the thick dotted line links the cores of the anion openings corresponding to those of the weakly dimerized donor molecules in the columnar stacks. In (d), the big and small open circles indicate anion openings around the cores corresponding to the hydrogen atoms which are situated closer to and further from the anion layer, respectively. See also footnote 30.

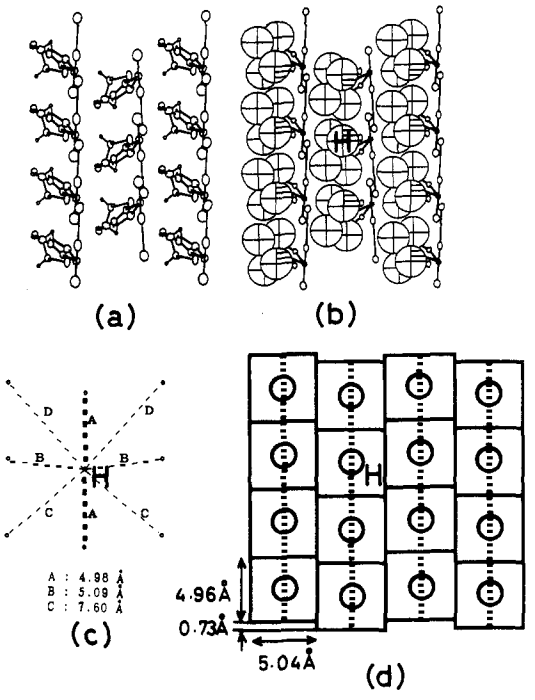


**Figure 9.** Crystal structure and pattern of the openings of the $\theta$-type BEDT-TTF salts. The anion layer projections of the crystal structures are illustrated for $\theta$-$(ET)_2I_3$ in (a) and (b). In (a) and (b), the occupancy of the $I_3$ ions is 0.5. In (c) and (d), the thick dotted line corresponds to the columnar stack of the donor molecules. See also footnote 30.

Summarizing the above discussion, each donor packing pattern exhibits a unique pattern of the cores at the anion openings. We propose that the pattern of the cores of the anion openings governs the donor packing motif in these BEDT-TTF salts.

**The Structural Factor Which Determines $T_c$.** A typical feature of the organic conductors is the large degree of freedom in the conducting and counter components. The size, the shape, and the formal charge of the component molecule can be controlled using methods of organic syntheses. Thus, a variety of crystal structures can be generated and a general structure–property relationship of the conducting material is difficult to conclude.

In the early stages of the discovery of BEDT-TTF superconductors, it was found that the bigger the unit cell volume, the higher the $T_c$ in a $\beta$-type salt.[37] Also, the relationship between the length of the trihalide anion and $T_c$ was examined to inspect the nature of the $\beta$-type salts.[38] Corresponding to the development of the various types of the BEDT-TTF superconductors, the concept of the effective volume ($V_{eff}$) was proposed.[1,7] This concept evolved from the idea that a low density of the BEDT-TTF molecules in the crystal induces a narrow bandwidth and high density of states at the Fermi level. This causes a high $T_c$.

As previously described, a linear correlation between $V_{eff}$ and $T_c$ was observed for several ambient-pressure BEDT-TTF superconductors having different shaped anions. $V_{eff}$ ranged from 693 Å$^3$ for $\beta$-$(ET)_2IBr_2$ to 714 Å$^3$ for $\kappa$-$(ET)_2Cu(NCS)_2$ corresponding to $T_c$'s of 2.7 to 10.4 K, respectively. However, the estimation of $V_{eff}$ leads to significant errors since the anion is roughly approximated as a cylinder with the radius of the biggest anion atom. This naive definition results in ambiguity in the value of $V_a$. Hence, there is also a large uncertainty in the value of $V_{eff}$. For example, for $\kappa$-$(ET)_2Cu[N(CN)_2]Br$, $V_{eff}$ is calculated to be 15 Å$^3$ smaller than when it is assumed that the C–N vdW is equal to the carbon atom radius. The difference of $V_{eff}$ corresponds to that of the $T_c$ of ca. 5 K. Also the choice of the van der Waals radius (after Pauling[39] or after Bondi[40]) affects the values of $V_a$, $V_{eff}$, and the estimated $T_c$.

To avoid ambiguity in $V_{eff}$, we need to calculate the volume of space which participates in electrical conduction in the crystal using clearly defined values. An improved method to estimate the effective volume is discussed below.

On the basis of the fact that BEDT-TTF superconductors show two-dimensional conducting properties,[1,41] the crystallographic unit cell can be divided in three parts. We defined the "most effective space" for the carrier distribution as the space which contains both the $C_6S_8$ skeleton of BEDT-TTF and an intra-donor-layer overlap space between the atomic orbitals belonging to the $C_6S_8$ $\pi$-system. The shape of this portion is sheetlike and parallel to the donor layer having a finite thickness. The "anion space" is defined as the space occupied by anion atoms. The carrier distribution does not occupy this space because the anion has a closed-shell electronic structure. The remainder part of the unit cell is classified as "secondary effective space" which includes donor ethylene groups and the anion openings. This part is sandwiched by the two "most effective spaces" and contributes to the carrier distribution less than the "most effective space".

To simplify the calculation, the "most effective space" is approximated by a parallelepiped having the same base area as

(37) Williams, J. M.; Beno, M. A.; Wang, H. H.; Geiser, U. W.; Emge, T. J.; Leuing, P. C. W.; Crabtree, G. W.; Carlson, K. D.; Azevedo, L. J.; Venturini, E. L.; Schirber, J. E.; Kwak, J. F.; Whangbo, M.-H. *Physica B* **1986**, *136*, 371.

(38) Kistenmacher, T. J. *Solid State Commun.* **1987**, *63*, 977.

(39) Gordon, A. J.; Ford, R. A. *The Chemist's Companion, A Handbook of Practical Data, Technique, and References*; John Wiley & Sons: New York, 1972; p 109.

(40) Bondi, A. *J. Phys. Chem.* **1964**, *68*, 441.

(41) Saito, G.; Yamochi, H.; Nakamura, T.; Komatsu, T.; Ishiguro, T.; Nogami, Y.; Ito, Y.; Mori, H.; Oshima, K.; Nakashima, M.; Uchida, S.; Takagi, H.; Kagoshima, S.; Osada, T. *Synth. Met.* **1991**, *41–43*, 1993.

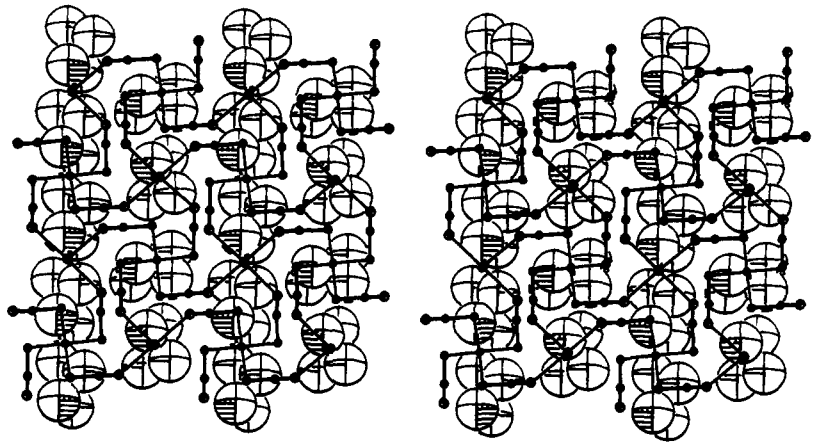

**Figure 10.** Stereoview of the anion layer projections of the ethylene hydrogen atoms and the anion atoms of $\alpha$-$(ET)_2NH_4Hg(SCN)_4$. The hydrogen atoms are drawn as spheres with a 1.2-Å radius, and the ones which are located closest to the anion layer are shaded. Only the nitrogen atoms are depicted for the ammonium ions.

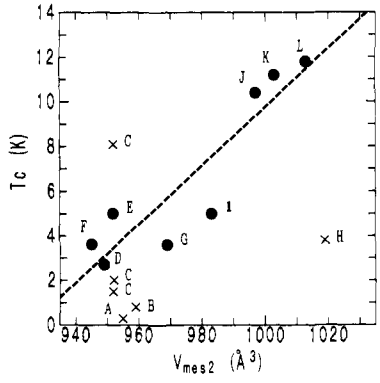


**Figure 11.** Plot of $V_{mes2}$ versus $T_c$ for $(BEDT\text{-}TTF)_2X$. Key: (A) $\alpha$-$(ET)_2KHg(SCN)_4$; (B) $\alpha$-$(ET)_2NH_4Hg(SCN)_4$; (C) $\beta$-$(ET)_2I_3$; (D) $\beta$-$(ET)_2IBr_2$; (E) $\beta$-$(ET)_2AuI_2$; (F) $\theta$-$(ET)_2I_3$; (G) $\kappa$-$(ET)_2I_3$; (H) $\kappa'$-$(ET)_2Cu_2(CN)_3$; (I) $\kappa$-$(ET)_2Ag(CN)_2{\cdot}H_2O$; (J) $\kappa$-$(ET)_2Cu(NCS)_2$; (K) $\kappa$-$(ET)_2Cu(CN)[N(CN)_2]$; (L) $\kappa$-$(ET)_2Cu[N(CN)_2]Br$. The dashed line indicates the result of the least-squares fit of the plot omitting the points A–C and H ($T_c$ (K) = $0.131V_{mes2}$ (Å$^3$) − 121).

the anion layer. Furthermore, we define the base of the parallelepiped as the plane parallel to the anion layer which contains the donor sulfur atom giving the shortest interlayer S··S distance through an anion opening.[42] The volume of the parallelepiped is calculated per two carries after the Cooper pair in the BCS theory and denoted as $V_{mes2}$. As shown in Figure 11 and Table IV, omitting $\alpha$-$(ET)_2MHg(SCN)_4$ (M = K, $NH_4$), $\kappa'$-$(ET)_2Cu_2(CN)_3$, and $\beta$-$(ET)_2I_3$, an almost linear relationship between $V_{mes2}$ and $T_c$ is observed for the ambient-pressure BEDT-TTF superconductors.

Limitations to approximating the geometry of the "most effective space" produce large deviations in the calculated values of $T_c$. The crystals of $\alpha$-$(ET)_2MHg(SCN)_4$ and $\kappa'$-$(ET)_2Cu_2(CN)_3$ contain a thick anion layer and disordered polar groups, respectively, both of which empirically lower $T_c$.[44] The plot of Figure 11 does not takes into account such effects. Concerning $\beta$-$(ET)_2I_3$, although the $V_{mes2}$ is calculated from the reported structural data at room temperature,[32] the structural parameters used are not appropriate. This salt shows incommensurate structural modulation below 195 K,[45] and the superconducting transition occurs at around 1.5 K (so called $\beta_L$-salt). Hence, the crystal structure around $T_c$ is different from that at room temperature. Also, this salt exhibits the $T_c$ values of 2.0 K[46] and 8.1 K (so called $\beta_H$-salt[47]) in the metastable states. Since these states survive only below 250 K, structural data at room temperature are not available.

Although the correlation between $V_{mes2}$ and $T_c$ is not perfect, $V_{mes2}$ contains ambiguity only from errors in the structural parameters. With omission of the above mentioned exceptions, using a least squares fit, $T_c$ is related to $V_{mes2}$ by the following equation:

$$T_c\,(\mathrm{K}) = 0.131V_{mes2}\,(\text{Å}^3) - 121$$

This relationship indicates that the physical constant of $T_c$ correlates strongly with parameter obtained from the crystal structure.

**Molecular and Crystal Design To Increase $T_c$ with a Planar Molecule.** Within the framework of BEDT-TTF superconductors discussed in this paper, it is noteworthy that the same area of the anion layer per donor molecule gives a bigger $V_{mes2}$ in the $\kappa$-modification than in the $\beta$-modification (Table IV). Therefore, $T_c$ of the $\kappa$-type salt is generally higher than that of the $\beta$-type one having the same area of the anion layer. For example, while $\beta$-$(ET)_2IBr_2$ and $\kappa$-$(ET)_2Cu(NCS)_2$ give the same area of 27.7 Å$^2$, the latter salt exhibits a bigger $V_{mes2}$ and higher $T_c$. We suggest that the $\kappa$-type salts are possible candidates to give high-$T_c$ BEDT-TTF superconductors. Concerning the effects on $T_c$ from the "secondary effective space" and the "anion space", we have only the empirical knowledge that the thinner ordered anion layer gives the higher $T_c$, as mentioned in the prvevious section. Combining these designing principles, we predict that the big and thin anions having the patterns of the openings indicated in Figure 5 will give $\kappa$-type BEDT-TTF superconductors with rather

(42) In $\kappa$-$(ET)_2Cu(CN)[N(CN)_2]$ and $\kappa'$-$(ET)_2Cu_2(CN)_3$, the lengths of the lines connecting the sulfur atoms which give the shortest interlayer S··S distances are 6.96 and 6.92 Å, respectively. However, these lines pass over the Cu atom and the bond in the disordered CN group in the anion layers, respectively. In these cases, the sulfur atoms which give the next-shortest interlayer S··S distances (6.98 and 7.03 Å, respectively) were adopted to define the bases of the parallelepipeds according to the definition. On the hand, it is noteworthy, even in $\alpha$-$(ET)_2NH_4Hg(SCN)_4$, which has the thickest and most complex anion layer in Table IV, the given line between the shortest interlayer S··S pair does not pass over the atoms or the bonds in the anion layer.

(43) Wang, H. H.; Beno, M. A.; Geiser, U.; Firestone, M. A.; Webb, K. S.; Nunez, L.; Crabtree, G. W.; Carlson, K. D.; Williams, J. M.; Azevedo, L. J.; Kwak, J. F.; Schirber, J. E. *Inorg. Chem.* **1985**, *24*, 2465.

(44) For the effects of the thickness of the anion layer, see ref 41. Although the conclusion is not free from criticism, the effect is also mentioned in: Harshman, D. R.; Mills, A. P., Jr. *Phys. Rev.* **1992**, *B45*, 10684. For the effect of disorder, see: Tokumoto, M.; Anzai, H.; Murata, K.; Kajimura, K.; Ishiguro, T.; *Jpn. J. Appl. Phys.* **1987**, *Suppl. 26*, 1977. Choi, M.-Y.; Chaikin, P. M.; Huang, S. Z.; Haen, P.; Engler, E. M.; Greene, R. L. *Phys. Rev.* **1982**, *B25*, 6208.

(45) Leuing, P. C. W.; Emge, T. J.; Beno, M. A.; Wang, H. H.; Williams, J. M.; Petricek, V.; Coppens, P. *J. Am. Chem. Soc.* **1985**, *107*, 6184.

(46) Kagoshima, S.; Hasumi, M.; Nogami, Y.; Kinoshita, N.; Anzai, H.; Tokumoto, M.; Saito, G. In *The Physics and Chemistry of Organic Superconductors*; Springer Proceedings in Physics Vol. 51; Saito, G., Kagoshima, S., Eds.: Springer-Verlag: Berlin, 1990; p 126.

(47) Creuzet, F.; Creuzet, G.; Jérome, D.; Schweitzer, D.; Keller, H. *J. Phys. Lett.* **1985**, *46*, L1079.

**Table IV.** Comparison of the Structural Features of $(BEDT\text{-}TTF)_2X$ Salts Having the Planar Anion Layers

| modification and Anion (X) | $T_c$,[a] K | inter-anion-layer dist, Å | area of anion layer/donor, Å$^2$ | shortest inter-layer S···S dist through an opening, Å | $V_{mes2}$, Å$^3$ |
|---|---|---|---|---|---|
| $\alpha$-$KHg(SCN)_4$ | <0.3 | 19.94 | 25.0 | 10.74 | 955 |
| $\alpha$-$NH_4Hg(SCN)_4$ | 0.8 | 19.98 | 25.1 | 10.74 | 959 |
| $\alpha$-$I_3$ | | 17.18 | 25.0 | 7.77 | 986 |
| $\beta$-$I_3$ | 1.5, 2, 8.1 | 15.07 | 28.2 | 6.75 | 952 |
| $\beta$-$IBr_2$ | 2.7 | 14.96 | 27.7 | 6.51 | 949 |
| $\beta$-$AuI_2$ | 5 | 15.17 | 27.8 | 6.82 | 952 |
| $\theta$-$I_3$ | 3.6 | 16.93 | 25.0 | 7.48 | 945 |
| $\kappa$-$I_3$ | 3.6 | 15.53 | 27.2 | 7.35 | 969 |
| $\kappa'$-$Cu_2(CN)_3$ | 3.8 | 14.84 | 28.5 | 7.03 | 1019 |
| $\kappa$-$Ag(CN)_2{\cdot}H_2O$ | 5.0 | 15.17 | 27.2 | 7.03 | 983 |
| $\kappa$-$Cu(NCS)_2$ | 10.4 | 15.24 | 27.7 | 7.13 | 997 |
| $\kappa$-$Cu(CN)[N(CN)_2]$ | 11.2 | 14.94 | 27.8 | 6.98 | 1003 |
| $\kappa$-$Cu[N(CN)_2]Br$ | 11.8 | 15.01 | 27.6 | 5.85 | 1013 |

[a] By four probe resistivity measurements, except $\beta$-$(ET)_2AuI_2$ for which $T_c$ was determined by the rf penetration method.[43]


**Figure 12.** Materialized candidate of the anion layer which will give $\kappa$-type BEDT-TTF salts. For example, M = transition metal and X = halogen anion or MX = neutral molecule. The shaded parts correspond to the openings.

high $T_c$'s. One of the materialized candidates which will give a $\kappa$-type salt is illustrated in Figure 12.

It is also noteworthy that the charge on the BEDT-TTF molecule is +0.5 in most of the ambient-pressure superconductors (see Table IV). Within the framework of the band calculation, $T_c$ may increase by adjusting the Fermi energy to the level of the maximum DOS. For example, $N(\epsilon_F)$ and hence $T_c$ of $\kappa$-$(ET)_2Cu(CN)[N(CN)_2]$ will be increased by the further oxidation of the donor molecule (see Figure 4).

Assuming the concept of $V_{mes2}$ is relevant to any component molecules, molecular designs can be achieved. To increase the thickness of the "most effective space" for the carrier distribution, a molecule with an elongated $\pi$-system is adequate. Furthermore, the component molecule must form a two-dimensional conducting layer. The vinylogs of the TTF molecule in which the central C=C moiety is extended satisfy these requirements and are expected to give high $T_c$ superconductors. The extension of the $\pi$-system to the periphery of the molecule will bring about not only an increase of the $V_{mes2}$ but also reinforced interactions between the conducting plane.

## Conclusion

The BEDT-TTF superconductors prepared by the electrocrystallization in the presence of Cu, CN, and $N(CN)_2$ have the $\kappa$-type crystal structures. Comparison of the relationship between the donor and the anion layers of these salts to those in the other ambient-pressure BEDT-TTF superconductors having the planar anion layers indicates that anion structure governs the donor packing motif. Namely, we have characterized a 1:1 correspondence between the modification and the pattern of the essential parts of the anion openings.

With revision of the method to estimate the volume of the space which contributes to the carrier distribution, the structural parameter of $V_{mes2}$ has been defined and derived solely from crystallographic parameters. The almost linear relationship between $T_c$ and $V_{mes2}$ indicates that the physical parameter of $T_c$ is strongly correlated with the structural parameter. This parameter corresponds to the volume of the space for the $C_6S_8$ skeletons of the donor molecules and the intra-donor-layer overlap space between them.

Concerning the effects on $T_c$ from the anion layer, we reconfirmed our working hypothesis that the thinner and bigger anion layer gives the higher $T_c$ for the BEDT-TTF superconductors. Also, it is suggested that the $\kappa$-type salts are more favorable than the $\beta$-type ones for the high-$T_c$ BEDT-TTF superconductors.

The analysis of the BEDT-TTF ambient-pressure superconductors has provided specific guiding principles to increase the $T_c$ of BEDT-TTF superconductors themselves. These principles may also be applied to seek new conducting component molecules for the organic superconductors using planar molecules.

**Acknowledgment.** The authors acknowledge Professor K. Toriumi for his kind advice on the orientation of the CN ion in the crystal. Also we thank Dr. A. Kobayashi, Dr. H. Mori, and Dr. G. C. Papavassiliou, who offered the unpublished structural data. This work was partly supported by a Grant-in-Aid for Science Research from the Ministry of Education, Science, and Culture of Japan and from The Sumitomo Foundation.

**Supplementary Material Available:** Tables listing the structural and thermal parameters of $\kappa$-$(BEDT\text{-}TTF)_2Cu(CN)[N(CN)_2]$ (Table S1) and $\kappa'$-$(BEDT\text{-}TTF)_2Cu_2(CN)_3$ (Table S2) and additional tables listing calculated coordinates of the ethylene hydrogen atoms (Tables S3–S13), distances between the cores of the anion openings (Tables S14–S16), and significant donor–anion atomic contacts (Table S17) for the BEDT-TTF salts included in Table IV (9 pages). Ordering information is given on any current masthead page.